# Multiband *d*-electron model for the photoemission spectrum of ultrathin magnetic overlayers

W. Z. Wang and K. L. Yao
*Department of Physics, Huazhong University of Science and Technology, Wuhan 430074, People's Republic of China*
(Received 11 December 2000; published 12 June 2001)

Many-body effect on the ground state and photoemission spectra of transition-metal/noble-metal overlayer is studied using multiband *d*-electron model and an exact diagonalization approach. A realistic band environment and the *d*-*d* intrasite interaction are considered. The results show that the many-body effect driven by the *d*-*d* interaction is qualitatively different from those of single-particle and single-band Hubbard models. With increasing interaction, four distinct ground states with different magnetization and particle occupation are obtained. The spin polarization of the photoemission spectrum is different in various ranges of the interaction. The spectral weight can be transferred between the states of different symmetries. The strong interaction can drive the hole from the transition-metal *d* orbitals to the noble-metal *s* orbitals and induce the spin polarization of the spectral weight by creating a noble-metal *s* hole.

DOI: 10.1103/PhysRevB.64.014415 PACS number(s): 75.10.Lp, 71.45.Gm, 79.60.−i

## I. INTRODUCTION

Ultrathin magnetic overlayers on various substrates may exhibit novel properties of interest to both fundamental studies of physics and potential new applications. Photoemission spectrum (PES) is one of the most frequently used experimental tools to measure the electronic structure of this matter.[1] Although theoretical understanding of the spectroscopy for ideal noninteracting and weekly interacting system is well established, it takes careful modeling, computation, and interpretation to understand the spectra of strongly correlated system such as 3*d* magnetic transition-metal systems and obtain correct physics. The magnitude of the Coulomb interaction between the *d* electrons in transition metal is close to, or in some cases even larger than, the *d*-band width. This strong electron-electron interactions invalidate the normal local-spin-density-approximation description[2–4] in some fundamental aspects. A well-known early example is the discovery[5] of the ''satellite'' peak in the photoemission spectrum of Ni and the subsequent theoretical explanation[6] of its many-body origin. Recently, various numerical schemes have been developed to study many-body effects in spectroscopic process in strongly correlated systems. These techniques may involve various approximations on the interaction terms.[7] However, a lot of recent work has focused on some ideal models, such as the single-band Hubbard model.[8,9] Sometimes it is necessary to include the orbital degeneracy and band-structure aspects in the model to correctly describe different physical phenomena. This is particularly true in the study of various spectroscopic behavior of highly correlated systems.

In this paper, we present the results of a theoretical study on the many-body effect on photoemission spectra of a realistic multiband *d*-electron model for transition-metal (TM)/noble-metal (NM) overlayer. Here the focus is on the effect of *d*-*d* Coulomb interactions. We do not intend to include all the details of the band structures in our model. Rather, we construct a generic *d*- and *s*-electron model to extract the fundamental physics involved. We study the effects of many-body strong correlation on the photoemission in a model system with realistic single-particle band structures. On one hand this model is simple enough to make the many-body problem fully tractable. On the other hand, both single-particle and many-body aspects of the problem are properly considered, allowing the extraction of interacting physics that is relevant for real materials systems. The calculated results show that the strong *d*-*d* Coulomb interactions produce different ground states with different spin and symmetries in the neutral state of the cluster. Some interesting results, including the spin polarization of the spectra and the transfer of hole between the TM and NM, have been observed.

The method used in this work is the periodic small-cluster approach.[10] It treats the band-structure effects and the electron-electron interaction on an equal footing. In this kind of approach, a model Hamiltonian that explicitly includes band-structure effects and many-body interactions is solved exactly. The problem is made tractable by modeling the sample as a finite-size crystal with periodic boundary conditions. This is equivalent to solving exactly a many-body problem with integrals in momentum space restricted to a finite sampling. Its advantage is that there is no approximation applied to the Hamiltonian. Quantum many-body problems are solved exactly in the numeric form. Therefore it provides accurate information about the many-body effect in the system. Its limitation is also obvious. Due to exponential growth of many-body states with the system size, only very small systems can be studied using this method. In practice, since many spectroscopic process are fast and intrinsically short ranged, they can be well described by the small-cluster approach. Numerous works on this subject have been reported. It has been successfully applied to various systems where local many-body effects are important: the photoemission behavior in bulk and surface Ni;[6(d),11] magnetic properties of bulk and surface Fe, Co;[12,13] electronic, magnetic, and superconducting properties of heavy-fermion system.[14–16] It is now generally accepted that the small-cluster approach provide rather accurate description of many interacting systems, although careful modeling and insightful interpretation of the calculated results are always required.

The rest of the paper is arranged as follows. Section II presents the model Hamiltonian and the method of calcula-

 

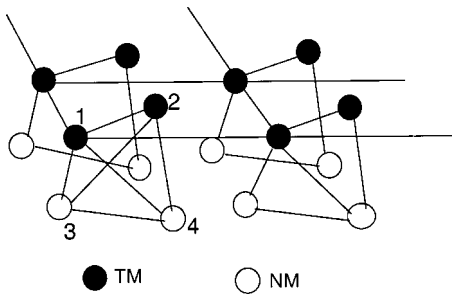


FIG. 1. The tetrahedral cluster in the two-layer fcc TM/NM(001) structure with periodic boundary conditions.

tion. In Sec. III, the properties of the ground state and the photoemission for different *d*-*d* interaction are calculated. The results and discussions are also given in Sec. III.

## II. THE MODEL HAMILTONIAN AND COMPUTATIONAL METHOD

In this work, we choose a tetrahedral cluster (see Fig. 1), the smallest nontrival fcc crystal, and apply periodic boundary conditions in two dimensions to construct the fcc TM/NM(001) structure, in which the two TM sites are in the top layer and two NM sites in the bottom layer. Only the interface NM layer is explicitly included to allow the electron (hole) hopping between the TM and NM sites. We only, explicitly, include the TM *d* and NM *s* orbitals and the nearest-neighbor interactions in the calculation.

The model Hamiltonian contains both single particle and interaction terms:

$$H=-\sum_{i,j;\mu,\nu;\sigma} t_{i\mu,j\nu}c^{\dagger}_{i\mu\sigma}c_{j\nu\sigma}+\sum_{i;\mu;\sigma} E_{\mu}c^{\dagger}_{i\mu\sigma}c_{i\mu\sigma}$$

$$+\sum_{i;\mu,\nu,\lambda,\phi;\sigma,\sigma'} V_{\mu\nu\lambda\phi}c^{\dagger}_{i\mu\sigma}c^{\dagger}_{i\nu\sigma'}c_{i\lambda\sigma'}c_{i\phi\sigma}, \qquad (1)$$

here $c^{\dagger}_{i\mu\sigma}$ ($c_{j\mu\sigma}$) denotes hole creation (annihilation) operator. The indices *i, j* label atoms in the cluster; $\mu$, $\nu$, $\lambda$, and $\phi$ label the TM *d* and NM *s* orbitals; $\sigma$ and $\sigma'$ are spin labels. The first-two terms are single-particle hopping and orbital-energy terms, and the third term describes the intraatomic interaction *on the TM sites only*. The single-particle parameters are obtained according to the Slater-Koster scheme.[17] In the following calculations we use a set of single-particle parameters based on previous work on some 3*d* transition-metal system:[18] $(dd\sigma)=1.0$ (its magnitude is chosen as the energy unit in the following calculation), $(dd\pi)=-0.8$, $(dd\delta)=0.2$, $(sd\sigma)=0.9$, $(ss\sigma)=2.0$, $E_{\alpha}=3.0$, $E_{\beta}=3.5$, $E_{\gamma}=2.8$, $E_{\delta}=E_{\epsilon}=3.4$, and $E_s=20$. The subscripts $\alpha$, $\beta$, $\gamma$, $\delta$, and $\epsilon$ refer to the five *d* orbitals of symmetry $r^2-3z^2$, $x^2-y^2$, $xy$, $yz$, and $zx$, respectively. $E_s$ labels the single-particle energy of *s* orbitals of noble metal. Three points are worth mentioning here. First, these are the renormalized parameters with only nearest-neighbor interactions among TM *d* orbitals and NM *s* orbitals explicitly included, not the ''bare'' band parameters as one would get in an all-electron single-particle tight-binding fit. Second, $E_s$ is much larger than other single-particle levels because the magnetization of the ground state is mainly contributed by 3*d* holes of TM and the NM does not provide *s* hole. Third, it should be pointed out that exact ratios of the single-particle parameters do not affect the qualitative physics studied in this work. In fact, we have tested several different sets of parameters; they all yield similar results.

The intraatomic interactions, which is the dominant contribution,[19] include three terms: a direct Coulomb integral *U* for two particles on the same *d* orbit, an exchange integral $J_{t_{2g}}$ for two particles on two different $t_{2g}$ orbitals, and another one $J_{e_g}$ for two particles on two different $e_g$ orbitals. The Coulomb interaction for two particles in different *d* orbitals is $U'=U-2J$. All intraatomic *d*-*d* interactions are expressed in terms of *U*, an average exchange integral $J=(J_{t_{2g}}+J_{e_g})/2$, and an exchange anisotropy $\delta J=(J_{e_g}-J_{t_{2g}})/2$. The interaction parameters are set in the ratios $U:J:\delta J=40:8:1$, based on the consideration of the constraints imposed by the atomic data and the screening effect in metals.[18] The fundamental physics extracted from the calculated results is insensitive to exact values of these ratios. This leaves *U* the only variable parameter in the present formulation. Below we will systematically study the effect of the *d*-*d* interaction *U* on the behavior of the photoemission.

With five *d* orbitals per TM atom per spin and one *s* orbital per NM atom per spin, there are 24 orbitals in the four-atom cluster for the TM/NM(011) structure. As an example we consider in the neutral state two *d* holes per TM atom and zero *s* hole per NM atom. Simple combinatorial arguments yield 10 626 many-body states in the neutral state of the cluster. The photoemission process introduces another hole, yielding 42 504 final states, respectively. The space and spin symmetries inherent in the Hamiltonian must be exploited in order to diagonalize the complete many-body Hamiltonian matrices. First, total spin and its *z* component in the cluster are good quantum numbers. Furthermore, space-group decomposition reduces the sizes of Hamiltonian matrices in a very efficient way. The cluster studied in this work have $C_4$ point group symmetry at the surface. The space group is the direct product of the $C_4$ group and the finite translational group of the periodic-cluster structure. There are eight irreducible representations, four at the $\Gamma$ and four at the *X* point. This corresponds to sampling the $\Gamma$ point, the center of the two-dimensional surface Brillouin zone, and the *X* point, the center of the zone boundary. All representations are nondegenerate. However, two pairs, $\Gamma_3$-$\Gamma_4$ and $X_3$-$X_4$, are degenerate due to time-reversal symmetry. With these representation the symmetrized basis functions are generated and then used to construct the Hamiltonian matrix that are in block-diagonalized form, partitioned according to various symmetry indices.[18] The largest Hamiltonian matrix is of order 2134, a significant reduction from the original order of 42 504. Direct diagonalization of these matrix provides exact solutions to the Hamiltonian.

## III. RESULTS AND DISCUSSIONS

The spin-resolved photoemission spectral function is defined as

TABLE I. Single-particle energy levels for TM/NM overlayer cluster [energies are in the unit of $(dd\sigma)$]. The symmetry corresponds to representations of space group. The degeneracy is per spin. The orbital is one of five *d* atomic orbitals.

| Energy | Degeneracy | Symmetry | orbital |
|---|---|---|---|
| −0.400 | 1 | $X_2$ | $\gamma$ |
| 0.300 | 1 | $\Gamma_2$ | $\beta$ |
| 1.400 | 1 | $X_1$ | $\alpha$ |
| 2.200 | 2 | $\Gamma_3$-$\Gamma_4$ | $\delta,\epsilon$ |
| 4.565 | 1 | $\Gamma_1$ | $\alpha$ |
| 4.600 | 2 | $X_3$-$X_4$ | $\delta,\epsilon$ |
| 6.000 | 1 | $\Gamma_2$ | $\gamma$ |
| 6.276 | 1 | $X_2$ | $\beta$ |
| 12.42 | 1 | $X_2$ | $s$ |
| 28.03 | 1 | $\Gamma_1$ | $s$ |

$$F_{PE}(\omega,\sigma)=\sum_{\mu,k}|\langle\phi_k^{N+1}|c_{\mu\sigma}^{\dagger}|\phi_0^N\rangle|^2\delta[\omega-(E_k^{N+1}-E_0^N)], \tag{2}$$

where $\phi_0^N$ and $\phi_k^{N+1}$ are the *N*-hole ground state and the *k*th $(N+1)$-hole final state, with energies $E_0$ and $E_k^{N+1}$, respectively. The operator $c_{\mu\sigma}^{\dagger}$ creates a hole with spin $\sigma$ on the orbital $\mu$. The calculated results are checked against the following sum rules:

$$\int F_{PE}(\omega,\sigma)\mathrm{d}\boldsymbol{\omega}=M-N_\sigma, \tag{3}$$

where $M$ is the total number of orbitals in the cluster and $N_\sigma$ is the total number of holes with spin $\sigma$ in the ground state of the *N*-hole system. This sum rule is satisfied in all reported cases.

In order to study the effect of the *d*-*d* Coulomb interaction $U$ on the photoemission spectra, we calculate the ground state in the neutral state with 4 holes. It is found that with increasing $U$ the ground states with different spins and symmetries can be obtained. Below we will find that the different photoemission spectra is actually due to different configurations of spin and symmetries of the ground state and the final states. When the interaction $U$ is turned off the total spin of the ground state is $S=0$. The calculated one-particle energy levels of the cluster are listed in Table I. Two holes with reverse spin occupy the $\beta$ orbitals and another two holes with reverse spin occupy $\gamma$ orbitals. The integrated PES of the cluster is shown in Fig. 2 for $U=0$. This is a single-particle spectrum without spin polarization. It is seen that there are five peaks located at different energy $E=E_0^N-E_k^{N+1}$, which is negative and its magnitude means the energy below the Fermi level or binding energy.[18] The first peak at about $E=-2.0$ is mainly contributed by the following three single-particle levels: twofold degenerate $\delta$ and $\epsilon$ orbitals with $E_{sl}=2.2$ and $\Gamma_3$-$\Gamma_4$ symmetry, and nondegenerate $\alpha$ orbital with $E_{sl}=1.40$ and $X_1$ symmetry. Here $E_{sl}$ labels the single-particle level. The second peak at about $E=-4.5$ results from $\alpha$ orbital with $E_{sl}=4.57$ and symmetry

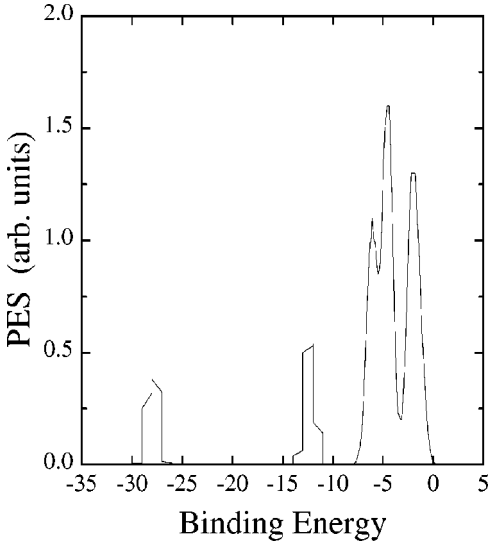


FIG. 2. The single-particle photoemission spectra ($U=0$), which is degenerate with respect to majority-spin and minority-spin.

$\Gamma_1$, and twofold degenerate $\delta$ and $\epsilon$ orbitals with $E_{sl}=4.60$ and symmetries $\Gamma_3$-$\Gamma_4$. The third peak at about $E=-6.0$ is originated from $\gamma$ orbital with $E_{sl}=6.00$ and symmetry $\Gamma_2$, and $\beta$ orbital with $E_{sl}=6.28$ and symmetry $X_2$. The fourth peak at $E=-12$ and the fifth peak at $E=-28$ are produced by the NM *s* orbitals with symmetry $X_2$ and $\Gamma_1$, respectively. From Fig. 2 we also find that the weight of the second peak is greater than the first peak although they should be nearly same actually. This is due to some overlap between the second peak and the third peak.

When the *d*-*d* interaction $U$ is turned on, but is weak (e.g., $U<3$) there is still no spin polarization in PES. In this case the many-body effect is weak and the PES exhibits the characteristics of single-particle spectrum since the interaction $U$ is much less than the single-particle bandwidth and the total spin of the neutral ground state is $S=0$. As the value of $U$ increases to 3.0, the total spin of the neutral ground state is $S=1$. Due to the interaction $U$, the hole occupying the majority-spin $\beta$ orbital transfers to the minority-spin $\alpha$ orbital. It predicts a spin polarization in the spectra since the numbers of holes with different spins are different in the ground state. The following sum rule of the relative polarization should hold in the PES calculations since the ratio of up- and down-spin states in the ground state should be 11/9 (three holes are in minority-spin levels of $\alpha$, $\beta$, and $\gamma$, and one hole is in majority-spin level of $\gamma$),

$$(I_+-I_-)/(I_++I_-)=(11-9)/(11+9)=10\%, \tag{4}$$

where $I_+$ and $I_-$ are the total intensities of the majority- and minority-spin states. Figure 3 presents the spin-resolved PES in this case. It is clearly seen that the spectral weight of the majority spin is greater than that of minority spin. To illustrate in more detail the many-body effects in PES, it is instructive to project the PES onto the spectral weight from various symmetries. The projected PES are shown in Fig. 4. One can see that the spin polarization in the integrated PES

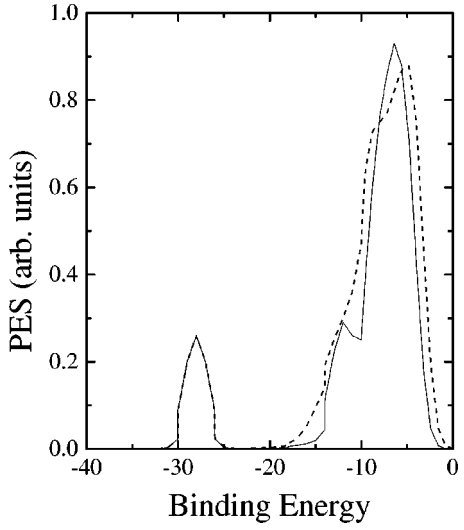


FIG. 3. The photoemission spectra for the interaction $U=3.0$. The solid and dashed lines represent minority-spin and majority-spin results, respectively.

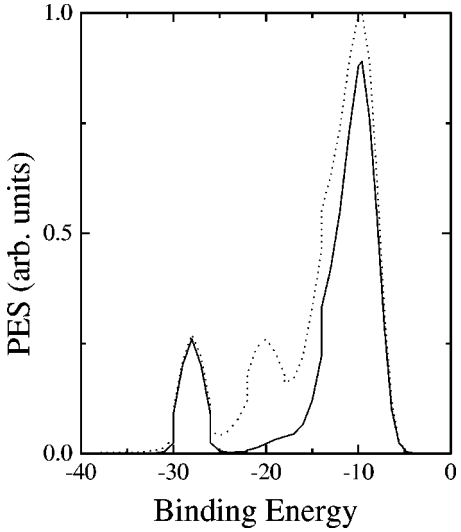


FIG. 5. The photoemission spectra for $U=7.0$. The solid and dashed lines represent minority-spin and majority-spin results, respectively.

comes from states of $\Gamma_2$ and $X_1$ symmetries. The spectral weight from $\Gamma_2$ states is fully spin polarized in majority-spin orientation. Comparing the PES for $U=0$ with those for $U=3$, it is found that the interaction $U$ drives the spectral weight from the $\Gamma_2$ states of minority spin to the $X_1$ states of majority spin. In the many-body approach, configuration interactions mix all single-particle energy levels. A full many-body picture is necessary to understand the photoemission results. The spectral weight of $\Gamma_2$ symmetry comes from creating a majority-spin hole with the mixed configuration of $\alpha$ and $\beta$ orbitals. The many-body states with mixture of orbitals $\alpha$, $\beta$, $\gamma$ leads to the spin-polarized spectra weight with $X_1$ symmetry. The spectral weights from the states of other symmetries are also spin resolved although these spectra weights with opposite spin are nearly the same. This is because the $d$-$d$ interaction splits the energy levels with opposite spin. It is noticeable that the spectral weight from the noble-metal $s$ orbital still exhibits the characteristics of single particle because its energy levels are deep and the configuration without NM $s$ holes in the ground state is kept. In the intergrated PES (Fig. 3), the position and the intensity of the spectral weight from NM $s$ orbitals are the same as those for $U=0$. However, its weights at $E=-12$ and $E=-28$ result from the states of $\Gamma_1$ and $X_2$ symmetry, respectively, which is different from the case of $U=0$. This is because that although the levels of $s$ orbitals are not changed, other $d$ orbitals are changed by the $d$-$d$ interaction and the configuration of many-body states that $s$ orbitals belong to is different from that in the case of $U=0$.

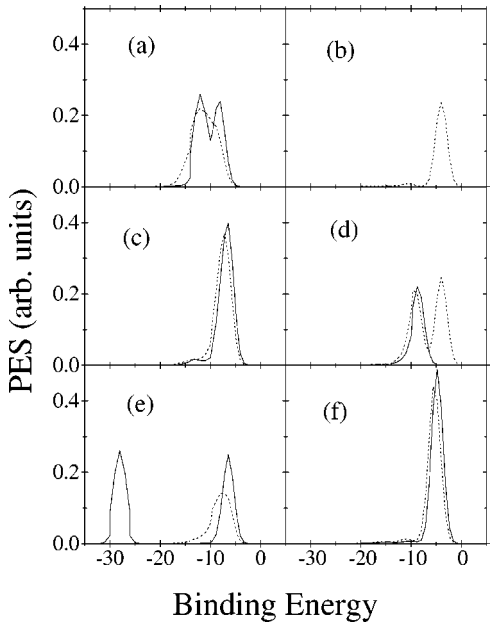


FIG. 4. The photoemission spectra projected onto different symmetry states for $U=3.0$. Results in (a)–(f) correspond to the symmetry $\Gamma_1$, $\Gamma_2$, $\Gamma_3$-$\Gamma_4$, $X_1$, $X_2$, and $X_3$-$X_4$. The solid and dashed lines represent minority-spin and majority-spin results, respectively.

As the interaction $U$ is enhanced continuously, but $U<7.0$, the total spin of the ground state is still $S=1$. The total spectral weights with majority spin and minority spin are the same as those in the case of $U=3.0$. The peaks are broaden and driven to higher bind energy by the interaction. When the $d$-$d$ interaction $U$ increases to 7.0, the ground state is fully polarized and its total spin is $S=2$. Comparing with the case of $U=3.0$, the hole occupying the majority-spin $\gamma$ orbital transfers to the minority-spin $\delta$ or $\epsilon$ orbital. The overall calculated relative spin polarization of the PES is 20% in the majority-spin orientation. However, it is not distributed homogeneously. From Fig. 5 we find that the spin polarization is very weak near the Fermi level, while that with higher binding energy is very high. The projected PES onto the states of different irreducible representations are shown in Fig. 6. In the part of PES close to $E=0$, the spectral weights from states of $\Gamma_1$, $X_1$, and $X_2$ symmetries are polarized in minority-spin orientation, while those from the states of $\Gamma_2$ and $X_3$-$X_4$ are polarized in majority-spin orientation. The

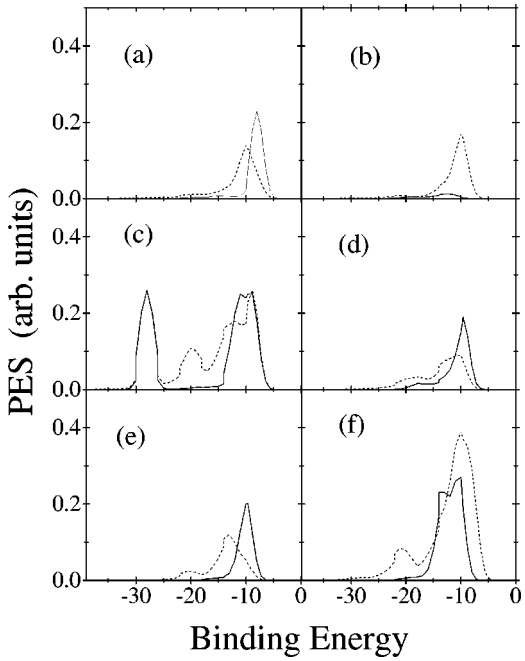


FIG. 6. The photoemission spectra projected onto different symmetry states for $U=7.0$. Other captions are the same as in Fig. 4.

combination of the contributions from states of various symmetries results in a very weak spin-polarized spectral weight in this part of the PES. This does not mean no many-body effect although it is weak in this part of the PES. It is worth noting that the spectral weight from states of $\Gamma_2$ is nearly full polarized in majority-spin orientation. This is because only the many-body states with the majority-spin holes introduced by PES process can match with the final states with symmetry $\Gamma_2$. In the main line of the PES, the part with higher binding energy is obviously spin polarized in majority-spin orientation. The second peak at $E=-20$ in Fig. 5 is almost fully polarized in majority-spin orientation and originated from the states of the symmetries $\Gamma_3$-$\Gamma_4$ and $X_3$-$X_4$. All these results show that the correlation effects caused by *d*-*d* interaction are quite strong. Comparing the PES for $U=7.0$ with the single-particle results we can study the interaction-driven spectral weight transfer between the states of different symmetries. The *d*-*d* interaction drives the spectral weight from the minority-spin $\Gamma_2$ and $X_2$ states toward the majority-spin $\Gamma_3$-$\Gamma_4$ and $X_3$-$X_4$ states. The spectral weights by creating NM *s* holes are not spin polarized and their position and intensity are conserved just as the case of weak interaction (e.g., $U=3.0$). However, these spectral weights are contributed by the many-body states with the symmetries $\Gamma_3$-$\Gamma_4$ and $X_3$-$X_4$, which are different from those in the case of $U=3.0$.

Because the single-particle levels of NM *s* orbital are very deep, the holes of the cluster avoid occupying these levels if the interaction $U$ is not strong enough. However, if the interaction $U>18$ the holes can be driven to the NM minority-spin *s* levels from the TM minority-spin *d* orbitals ($\epsilon$ or $\delta$ orbitals). The ground state is still fully polarized and has spin $S=2$. Figures 7 and 8 show the integrated PES and symmetry-projected PES for $U=20$. The feature of PES is

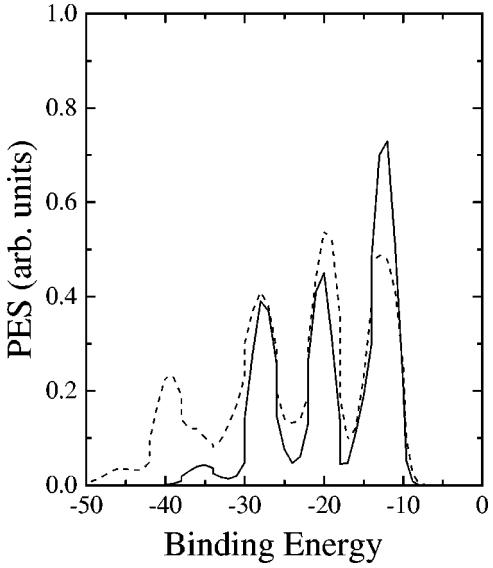


FIG. 7. The photoemission spectra for $U=20.0$. The solid and dashed lines represent minority-spin and majority-spin results, respectively.

quite different from those in the cases of weak interaction. There are four spin-resolved peaks that are highly spin polarized. The first peak in Fig. 7 is polarized in the minority-spin orientation, while other three peaks are polarized in the majority-spin orientation. The projected PES shows that the polarization is different with respect to different irreducible representations. The peak observed at about $E=-40$ is almost polarized in majority-spin orientation. This is a typical many-body effect caused by the reduced probability of creating two holes on the same orbital in that energy range. There is a significant amount of spectral weight beyond the range of single-particle levels. It is apparently driven by the

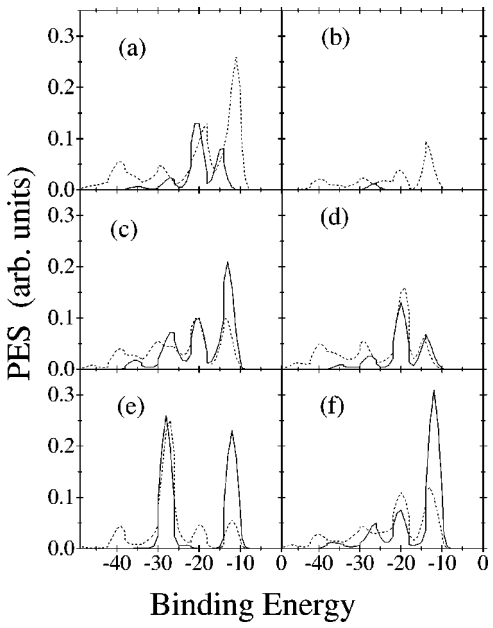


FIG. 8. The photoemission spectra projected onto different symmetry states for $U=20.0$. Other captions are the same as in Fig. 4.

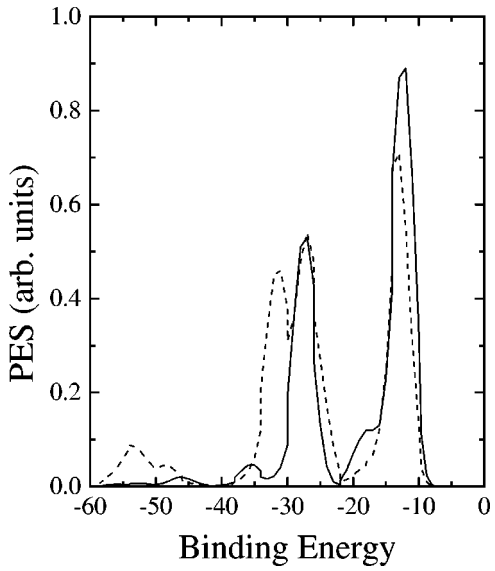


FIG. 9. The photoemission spectra for $U=30.0$. The solid and dashed lines represent minority-spin and majority-spin results, respectively.

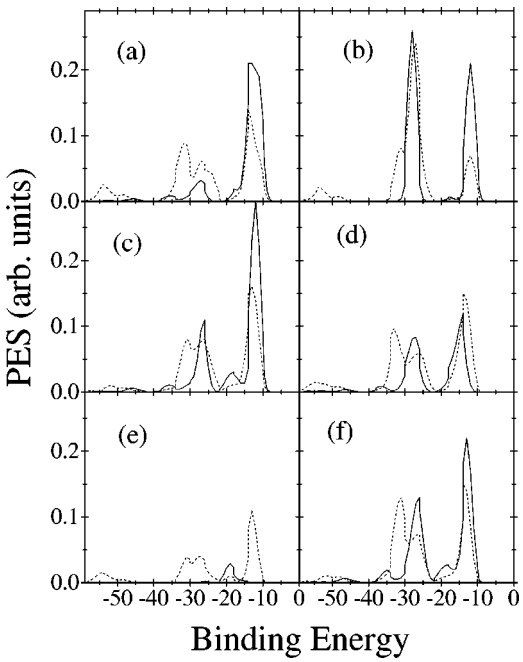


FIG. 10. The photoemission spectra projected onto different symmetry states for $U=30.0$. Other captions are the same as in Fig. 4.

*d*-*d* interaction. Comparing the present PES with the single-particle results, dramatic spectral weight transfer occurs. The spectral weight from the minority-spin $\Gamma_1$ and $\Gamma_2$ states is transferred to the majority-spin $\Gamma_1$ and $X_1$ states. From Fig. 8, it can be seen that the total number of spin-resolved peaks of various symmetries is much more than the number of single-particle levels. This is because there is so many configurations of many-body states in the ground states and the final states, and the strong interaction separates intensivly the energies of the final states with different configurations of many-body states. More interestingly, the spectral weight coming from the NM *s* orbitals is also spin-polarized because in the ground-state configuration nearly one NM *s* hole is in minority-spin states and thus majority-spin holes introduced by photoemission have higher probability to experience stronger interaction due to Pauli principle. The detailed study shows that this spin-polarized part of the spectral weight coming from *s* orbital is located at about $E=-12$ and originated from the states of symmetry $\Gamma_1$, while the nonpolarized part of the spectral weight at $E=-28$ results from the $X_2$ states.

When the *d*-*d* interaction increases to $U>29$, the holes of the system will transfer continuously from TM minority-spin $\beta$ orbitals to the NM majority-spin *s* orbitals. The total spin of the ground state becomes $S=1$. The relative spin polarization decreases to 10% in the majority-spin orientation. Moreover, the spin polarization is not evenly distributed. The integrated PES and the projected PES are shown in Figs. 9 and 10 for $U=30$. From Fig. 9, we find that the main line is spin polarized in the minority-spin orientation. This indicates that there is a higher probability of creating a minority-spin hole, in this range of energy, although most holes in the ground state have minority spin. The second peak is strongly polarized and the third peak is almost fully spin polarized in the majority-spin orientation. These results show a strong many-body effect and can be understood using the following explanation. Due to the *d*-*d* interaction the density of many-body states in the final states is not distributed uniformly with respect to spin configuration and energy. On the other hand, the configuration of many-body states in the ground state is not symmetric with respect to spin. Therefore, the probability of creating a hole with different spin in the different range of energy is different. It is noticeable that the spectral weight from the NM *s* orbitals is almost not polarized because in the ground-state configuration the numbers of hole occupying *s* orbitals with opposite spin are nearly the same. This part of the spectral weight is mainly contributed by the states of $\Gamma_1$ symmetry.

In summary, we have studied the PES of transition-metal/noble-metal overlayer using a multiband *d*-electron model. The many-body effect driven by the *d*-*d* interaction is qualitatively different from those of single-particle and single-band Hubbard models. The results show that there are four distinct ground states with various configurations of spin and hole occupation when the interaction *U* increases. As a result, the relative spin polarization of the PES by creating a hole from one of these ground states is different. This polarization is not evenly distributed in the different irreducible representations and different ranges of energy due to the strong correlation effect introduced by the *d*-*d* interaction. The symmetry-projected PES shows that the spectral weight transfer occurs between the states of different symmetries. When the interaction is strong enough the hole can transfer between the TM *d* orbitals and the NM *s* orbitals. The combination of this *s*-*d* hybridization and *d*-*d* interaction results in the spin polarization of the spectral weight by creating a NM *s* hole. It is noticeable that some quantitative changes

are expected as the parameters in Hamiltonian vary. However, we want to emphasize the qualitative physics involved here, i.e., the spin polarization of the PES and the spectral transfer are driven by the *d*-*d* interaction in a realistic-band environment. Our conclusion should not be affected in any fundamental way. Further work will be carried out to study in detail the *s*-*d* hybridization effect for understanding and interpreting the PES.

**ACKNOWLEDGMENTS**

One of authors (W.Z. Wang) would like to thank Dr. C. Chen for his help with the computer codes at the early stages of this work. This research was supported partly by the National Science Foundation of China under Grant No. 10004004, and partly by the Foundation of Ministry of Education of China.

[1] See, for example, F.J. Himpsel, Adv. Phys. **32**, 1 (1983); Comments Condens. Matter Phys. **12**, 199 (1986).
[2] C.S. Wang, B.M. Klein, and H. Krakauer, Phys. Rev. Lett. **54**, 1852 (1985).
[3] J. Chen, D. Singh, and H. Krakauer, Phys. Rev. B **38**, 12 834 (1988).
[4] E.D. Fabrizio, G. Mazzone, C. Petrillo, and F. Sacchetti, Phys. Rev. B **40**, 9502 (1989).
[5] L.A. Feldkamp and L.C. Davis, Phys. Rev. Lett. **43**, 151 (1979); W. Eberhardt and E.W. Plummer, Phys. Rev. B **21**, 3245 (1980).
[6] (a) D.R. Penn, Phys. Rev. Lett. **42**, 921 (1979); (b) A. Liebsch, *ibid.* **43**, 1431 (1979); (c) R. Clauberg, Phys. Rev. B **28**, 2561 (1983); (d) R.H. Victora and L.M. Falicov, Phys. Rev. Lett. **55**, 1140 (1985).
[7] M.M. Steiner, R.C. Albers, and L.J. Sham, Phys. Rev. B **45**, 13 272 (1992).
[8] E. Dagotto, Rev. Mod. Phys. **66**, 763 (1994), and references therein.
[9] J. Zheng and C. Chen, Phys. Rev. B **51**, 14 092 (1995).
[10] L. M. Falicov, in *Recent Progress in Many-body Theories*, edited by E. Pajanne and R. Bishop (Plenum, New York, 1988), Vol. I, p. 275, and references therein.
[11] C.F. Chen and L.M. Falicov, Phys. Rev. B **40**, 3560 (1989).
[12] E.C. Sowa and L.M. Falicov, Phys. Rev. B **35**, 3765 (1987).
[13] E.C. Sowa and L.M. Falicov, Phys. Rev. B **37**, 8707 (1988).
[14] A. Reich and L.M. Falicov, Phys. Rev. B **37**, 5560 (1988).
[15] A. Reich and L.M. Falicov, Phys. Rev. B **38**, 11 199 (1988).
[16] C.F. Chen, A. Reich, and L.M. Falicov, Phys. Rev. B **38**, 12 823 (1988).
[17] J.C. Slater and G.F. Koster, Phys. Rev. **94**, 1498 (1954).
[18] C. Chen, Int. J. Mod. Phys. B **5**, 1147 (1991), and references therein; C. Chen, Phys. Rev. B **45**, 13 811 (1992); **48**, 1318 (1993).
[19] C. Herring, in *Magnetism*, edited by G. T. Rado and H. Suhl (Academic, New York, 1966), Vol. 4.